Dissipative Effects in Hydromagnetic Boundary Layer Nanofluid Flow past a Stretching Sheet with Newtonian Heating

B. K. Mahatha[1], R. Nandkeolyar[2†], G. K. Mahto[3] and P. Sibanda[4]

[1] *Department of Mathematics, School of Applied Sciences, KIIT University, Bhubaneswar-751024, India*
[2] *School of Mathematics, Thapar University, Patiala-147004, India*
[3] *Department of Mathematics, Centurion University of Technology & Management, Bhubaneswar-752050, India*
[4] *School of Mathematics, Statistics & Computer Science, University of KwaZulu-Natal, Private Bag X01, Scottsville 3209, Pietermaritzburg, South Africa*

Email: *rajnandkeolyar@gmail.com*

ABSTRACT

Two dimensional steady hydromagnetic boundary layer flow of a viscous, incompressible, and electrically conducting nanofluid past a stretching sheet with Newtonian heating, in the presence of viscous and Joule dissipations is studied. The transport equations include the combined effects of Brownian motion and thermophoresis. The governing nonlinear partial differential equations are transformed to a set of nonlinear ordinary differential equations which are then solved using Spectral Relaxation Method (SRM) and the results are validated by comparison with numerical approximations obtained using the Matlab in-built boundary value problem solver bvp4c, and with existing results available in literature. Numerical values of fluid velocity, fluid temperature and species concentration are displayed graphically versus boundary layer coordinate for various values of pertinent flow parameters whereas those of skin friction, rate of heat transfer and rate of mass transfer at the plate are presented in tabular form for various values of pertinent flow parameters. Such nanofluid flows are useful in many applications in heat transfer, including microelectronics, fuel cells, pharmaceutical processes, and hybrid-powered engines, engine cooling/vehicle thermal management, domestic refrigerator, chiller, heat exchanger, in grinding, machining and in boiler flue gas temperature reduction.

NOMENCLATURE

a	constant associated with linear stretching	Le	Lewis number
B_0	applied magnetic field	M	magnetic parameter
Bi	Biot number	Nb	Brownian motion parameter
C	nanoparticle volume fraction	Nt	thermophoresis parameter
C_f	skin-friction coefficient	Nu_x	local Nusselt number
c_p	specific heat at constant pressure	Pr	Prandtl number
C_w	wall nanoparticle volume fraction	q_m	wall mass flux
C_∞	ambient nanoparticle volume fraction	q_w	wall heat flux
D_B	Brownian diffusion coefficient	Sh_x	local Sherwood number
D_T	thermophoretic diffusion coefficient	T	nanofluid temperature
Ec	Eckert number	T_f	characteristic temperature
f	dimensionless stream function	T_∞	ambient temperature of nanofluid
h	heat transfer coefficient	u	velocity component along x direction
k	thermal conductivity of the base fluid	u_w	stretching velocity of the sheet

v	velocity component along y direction		ϕ	dimensionless nanoparticle volume fraction
x	coordinate along the sheet		ψ	stream function
y	coordinate normal to the sheet		ρ	density of the base fluid
			σ	electrical conductivity of the base fluid
α	thermal diffusivity of base fluid		θ	dimensionless temperature
η	similarity variable		τ	ratio of specific heat capacities
μ	viscosity of the base fluid		τ_w	surface shear stress
ν	kinematic viscosity of the base fluid			

1. INTRODUCTION

Nanofluids have many applications in industries since materials of nanometer size have unique thermo-physical properties. The term "nanofluid" has been foremost introduced by Choi (1995). Basically, nanofluids are solid-liquid composite materials consisting of solid nanoparticles (or nanofibers with sizes typically of 1-50 nm) suspended in liquid. Nanofluids have attracted great interest recently because of reports of greatly enhanced thermal properties. A small amount ($< 1\%$ volume fraction) of Cupper (Cu) nanoparticles or carbon nanotubes dispersed in ethylene glycol or oil is reported to increase the inherently poor thermal conductivity of the liquid by 40% and 150% respectively (Choi *et al.* 2001). Thus, the performance of heat transfer systems can be significantly improved if regular fluids are replaced by nanofluids. The interdisciplinary nature of nanofluid research presents a great opportunity for exploration and discovery at the frontiers of nanotechnology. A comprehensive study of heat transfer in nanofluids was made by Buongiorno and Hu (2005), Kakac and Pramuanjaroenkij (2009), Das and Choi (2009), Wang and Mazumdar (2007) and Das *et al.* (2008). Due to the significance of the study of flow and heat transfer caused by a stretching surface in many practical manufacturing process e.g. drawing, annealing and tinning of copper wires, continuous stretching, rolling and manufacturing of plastic films and artificial fibers, heat treated materials traveling on conveyer belts, glass blowing, crystal growing, paper production, flow of fluids over stretching sheet was studied by a number of researchers. Sakiadis (1961) was the first one to analyze the boundary layer flow over a continuous solid surface moving with constant speed. Erickson *et al.* (1966) extended his study by including the wall suction or blowing and investigated its effects on the heat and mass transfer in the boundary layer. It was Crane (1970) who first studied the flow of an incompressible viscous fluid over a linearly stretching sheet. He obtained an exact solution for the flow field. Many researchers like Gupta and Gupta (1977), Grubka and Bobba

(1985), Cortell (2005), Chen (1998), Vajravelu and Roper (1999) studied the fluid flow over a stretching sheet considering different aspects of the problem. Though the use of a magnetic field provides a stabilization mechanism in fluid flow and heat transfer problems, the effect of applied magnetic field was not considered in the research studies made above. Such types of flows are encountered in polymer industry and metallurgy. The metallurgical applications include the cooling of continuous strips or filaments in, e.g., the process of drawing, annealing, and thinning of copper wires. However there are very few studies which consider the effect of an external magnetic field on the flow of a nanofluid over a stretching/shrinking sheet. The effect of magnetic field on stagnation point flow and heat transfer due to nanofluid towards a stretching sheet was studied by Ibrahim *et al.* (2013). Chamkha et al. Chamkha *et al.* (2011) investigated the unsteady, laminar, boundary-layer flow with heat and mass transfer of a nanofluid along a horizontal stretching plate in the presence of a transverse magnetic field, melting and heat generation or absorption effects. Mahapatra and Gupta (2001) and Mahapatra and Gupta (2002) and Mahapatra *et al.* (2009) investigated the magnetohydrodynamic stagnation point flow towards a stretching sheet. The two important features of nanofluids are Brownian motion and thermophoresis (Xuan and Li 2003). Brownian motion describes the random movement of nanoparticles in the base fluid. This random movement implies a collision of particles into each another. The collision passes on the kinetic energy of the particles to the molecules. The impact of particles upon other particles is negligible because the concentration of particles in nanofluids is normally low. Thermophoresis describes the nanoparticle dispersion in the base fluid due to temperature gradient. Nield and Kuznetzov (2009) studied the Cheng-Minkowycz problem for boundary layer flow of a nanofluid with Brownian motion and thermophoresis effects. The boundary layer flow of a nanofluid past a vertical flat plate has been discussed by Kuznetsov and Nield (2010). Khan and Pop (2010) investi-

gated the effects of Brownian motion and thermophoresis on boundary layer flow of nanofluid over a stretching sheet. Mustafa *et al.* (2011) reported a numerical solution for thermal boundary layer of a nanofluid in the region of stagnation point towards a stretching sheet. Makinde and Aziz (2011) presented an analysis of the thermal boundary layer of a nanofluid past a linearly stretching sheet with a convective surface boundary condition. Contributions on the flow of nanofluids are also due to Sreenivasulu and Bhaskar Reddy (2015), Parasuraman and Chellasamy (2015), Malvandi *et al.* (2014a) and Malvandi *et al.* (2014b).

Viscous and Joule dissipation effects are important in a number of fluid engineering devices. The energy dissipated due to motion of the fluid and retardation due to the application of magnetic field into the system, has a heating/cooling effect on the surface which result in significant heat transfer to the fluid in the boundary layer region. The hydromagnetic nanofluid flow due to a stretching/shrinking sheet with viscous dissipation and chemical reaction effects was studied by Kameswaran *et al.* (2012). They used the nanoparticle volume fraction model to describe the nanofluid flow problem. Hady *et al.* (2012) investigated radiation effect on the viscous flow of a nanofluid and heat transfer over a nonlinearly stretching sheet. Khan *et al.* (2012) studied the unsteady free convective boundary layer flow of a viscous, incompressible nanofluid along a stretching sheet with thermal radiation and viscous dissipation effects in the presence of an external transverse magnetic field. There are several industrial situations where the surface is convectively heated by external source. This causes a certain change in the surface temperature gradient and affects the temperature of the fluid within the boundary layer. Makinde and Aziz (2011) investigated the boundary layer flow induced in a nanofluid due to a linearly stretching sheet. They included the effects of Brownian motion and thermophoresis effects in the governing transport equation. Ibrahim and Shanker (2012) studied the boundary layer flow and heat transfer of nanofluid over a vertical plate with Newtonian heating. The investigation of boundary layer stagnation point flow of a nanofluid past a permeable flat surface with Newtonian heating was carried by Olanrewaju and Makinde (2013). They used the Brownian motion and thermophoresis effects to model the nanofluid flow. Recently, Nandkeolyar *et al.* (2013) investigated the effects of viscous and Joule heating in the MHD stagnation point flow through a stretching sheet in the pres-

ence of homogeneous-heterogeneous reactions and non-linear convection.

The aim of the present study is to investigate the steady hydromagnetic boundary layer flow of a viscous, incompressible, and electrically conducting nanofluid past a stretching sheet. The effects of dissipative heat transfer due to viscous and Joule dissipations are taken into consideration. The surface of the stretching sheet is convectively heated with a hot fluid which results in the Newtonian heating effect into the system. The Brownian motion and thermophoretic effects are taken into account to model the nanofluid flow. Such flow model finds applications in high-viscosity fluid engineering devices which work under the influence of an external magnetic field.

2. FORMULATION OF THE PROBLEM

Consider a steady two dimensional boundary layer flow of a viscous, incompressible, and electrically conducting nanofluid over a stretching surface (at $y = 0$) that is subjected to a Newtonian heating process, which is characterized by a temperature T_f and a heat transfer coefficient h. Let the x- axis be taken along the surface and y- axis normal to it. The fluid flow is induced due to the stretching velocity $u_w(x)$ of the sheet along x-axis while the fluid outside the boundary layer is at rest. The fluid flow is permeated with a uniform transverse magnetic field B_0 applied parallel to y-axis. No applied or polarized voltages exist so the effect of polarization of fluid is negligible. This corresponds to the case where no energy is added or extracted from the fluid by electrical means (Meyer 1958). It is assumed that induced magnetic field generated by fluid motion is negligible in comparison to the applied one. This assumption is justified because magnetic Reynolds number is very small for liquid metal and partially ionized fluids (Cramer and Pai 1973). The nanoparticle volume fraction C and nanofluid temperature T at the surface are C_w and T_w, respectively, while these values outside the boundary layer region, are C_∞ and T_∞, respectively.

Under the assumptions made above the boundary layer equations governing the conservation of mass, momentum, energy and nano particle volume fraction can be written as (Cramer and Pai 1973; Mustafa *et al.* 2011; Makinde and Aziz 2011; Nandkeolyar *et al.* 2013)

$$\frac{\partial u}{\partial x} + \frac{\partial v}{\partial y} = 0, \tag{1}$$

$$u\frac{\partial u}{\partial x} + v\frac{\partial u}{\partial y} = \nu\frac{\partial^2 u}{\partial y^2} - \frac{\sigma B_0^2}{\rho}u, \tag{2}$$

$$u\frac{\partial T}{\partial x} + v\frac{\partial T}{\partial y} = \alpha\frac{\partial^2 T}{\partial y^2} + \tau\left[D_B\frac{\partial C}{\partial y}\frac{\partial T}{\partial y} + \frac{D_T}{T_\infty}\left(\frac{\partial T}{\partial y}\right)^2\right]$$
$$+ \frac{\mu}{\rho c_p}\left(\frac{\partial u}{\partial y}\right)^2 + \frac{\sigma B_0^2}{\rho c_p}u^2, \tag{3}$$

$$u\frac{\partial C}{\partial x} + v\frac{\partial C}{\partial y} = D_B\frac{\partial^2 C}{\partial y^2} + \frac{D_T}{T_\infty}\frac{\partial^2 T}{\partial y^2}, \tag{4}$$

where u and v are velocity components in x and y directions, respectively, ν is kinematic coefficient of viscosity, σ is electrical conductivity, ρ is density, T is temperature, α is thermal diffusivity, $\tau = \frac{(\rho c)_p}{(\rho c)_f}$ is the ratio of effective heat capacity of the nanoparticle material and heat capacity of the fluid, D_B is Brownian diffusion coefficient, D_T is thermophoretic diffusion coefficient, μ is dynamic viscosity, c is specific heat at constant pressure. The subscripts p and f stand for the thermophysical properties of nanoparticles and the base fluid, respectively.

The governing Eqs. (1)-(4) constitute the equations governing the conservation of mass, momentum, heat and nanoparticle volume fraction. The first two terms in the left hand side of Eq. (2) presents the effect of inertial forces while the first and second terms in the right hand side account for the effects of viscous and Lorentz forces, respectively. The second and third terms in the right hand side of Eq. (3) incorporate the effects of Brownian diffusion and thermophoretic diffusion, respectively while the last two terms in this equation are due to dissipative heat transfer caused due to viscous and Joule dissipations. Equation (4) which governs the conservation of nanoparticle volume fraction also considers the effect due to Brownian diffusion and thermophoretic diffusion (see last two terms in Eq. (4)).

The boundary conditions for the problem are

$$u = u_w(x) = ax, \ v = 0, \ -k\frac{\partial T}{\partial y} = h(T_f - T),$$

$$C = C_w \text{ at } y = 0$$
$$u = 0, \ v = 0, \ T = T_\infty, \ C = C_\infty, \text{ as } y \to \infty \tag{5}$$

where k is thermal conductivity of the nanofluid.

We now introduce the following transforma-

tions

$$\psi(x,y) = \sqrt{a\nu}xf(\eta), \ \theta = \frac{(T - T_\infty)}{(T_f - T_\infty)},$$

$$\phi = \frac{(C - C_\infty)}{(C_w - T_\infty)}, \ \eta = \sqrt{\frac{a}{\nu}}y, \tag{6}$$

where η is similarity variable, $\psi(x,y)$ is the stream function, and $f(\eta)$ is the dimensionless stream function. The above transformation is chosen in such a way that $u = \partial\psi/\partial y$ and $v = -\partial\psi/\partial x$.

Using the above transformation, the equation of continuity (1) is automatically satisfied and we obtain from Eqs. (2), (3) and(4), respectively as

$$f''' + ff'' - f'^2 - Mf' = 0 \tag{7}$$
$$\theta'' + Prf\theta' + PrNb\ \phi'\theta' + PrNt\theta'^2$$
$$+ PrEcf''^2 + PrMEcf'^2 = 0 \tag{8}$$
$$\phi'' + Lef\phi' + \frac{Nt}{Nb}\theta'' = 0 \tag{9}$$

subject to the following boundary conditions:

$$f = 0, \ f' = 1, \ \theta' = -Bi[1 - \theta], \ \phi = 1 \text{ at } \eta = 0$$
$$f' \to 0, \ \theta \to 0, \ \phi \to 0 \text{ as } \eta \to \infty, \tag{10}$$

In the above equations, primes denote differentiation with respect to η and the seven parameters are defined by

$$M = \frac{\sigma B_0^2}{\rho a}, \ Pr = \frac{\nu}{\alpha}, \ Nb = \frac{(\rho c)_p D_B(c_w - c_\infty)}{(\rho c)_f \nu},$$

$$Nt = \frac{(\rho c)_p D_T(T_f - T_\infty)}{(\rho c)_f T_\infty \nu}, Ec = \frac{u^2}{c_p(T_f - T_\infty)},$$

$$Le = \frac{\nu}{D_B}, \ Bi = \frac{h}{k}\sqrt{\frac{\nu}{b}},$$

where M is the magnetic parameter, Pr is the Prandtl number, Nb is the Brownian motion parameter, Nt is the thermophoresis parameter, Ec is the Eckert number, Le is the Lewis number, and Bi is the Biot number.

The physical quantities of interest are the skin friction coefficient C_f, the local Nusselt number Nux and the local Sherwood number Shx which are defined as

$$C_f = \frac{\tau_w}{\rho U_\infty^2}, \ Nu_x = \frac{xq_w}{k(T_f - T_\infty)},$$

$$Sh_x = \frac{xq_m}{D_B(C_w - C_\infty)}$$

where the surface shear stress τ_w, the local heat flux q_w, and the local mass flux q_m are given by

$$\tau_w = \mu \left(\frac{\partial u}{\partial y} \right)_{y=0}, \quad q_w = -k \left(\frac{\partial T}{\partial y} \right)_{y=0},$$

$$q_m = -D_B \left(\frac{\partial C}{\partial y} \right)_{y=0}$$

Using the similarity variables (6), the coefficients of skin-friction, heat transfer, and mass transfer, are given by

$$(Re_x)^{1/2} C_f = f''(0), \tag{11}$$

$$(Re_x)^{-1/2} Nu_x = -\theta'(0), \tag{12}$$

$$(Re_x)^{-1/2} Sh_x = -\phi'(0) \tag{13}$$

where $Re_x = \frac{u_w x}{\nu}$ is the local Reynolds number.

3. SOLUTION TECHNIQUE

In order to solve the equations (7)-(9) subject to the boundary conditions (10) the Spectral Relaxation Method (SRM) suggested by Motsa and Makukula (2013) and Kameswaran *et al.* (2013) is used. The method uses the Gauss-Seidel approach to decouple the system of equations. In the framework of SRM method the iteration scheme is obtained as

$$f'_{r+1} = p_r, \quad f_{r+1}(0) = 0, \tag{14}$$

$$p''_{r+1} + f_{r+1} p'_{r+1} - M p_{r+1} = p_r^2, \tag{15}$$

$$\theta''_{r+1} + Pr f_{r+1} \theta'_{r+1} = -[Pr Nb \theta'_r \phi'_r + PrNt \theta'^2_r$$
$$+ PrEc \, p'^2_{r+1} + PrMEc \, p^2_{r+1}], \tag{16}$$

$$\phi''_{r+1} + Le f_{r+1} \phi'_{r+1} = -\frac{Nt}{Nb} \theta''_{r+1}, \tag{17}$$

The boundary conditions for the above iteration scheme are

$$p_{r+1}(0) = 1, \quad p_{r+1}(\infty) \to 0, \tag{18}$$

$$\theta'_{r+1}(0) = -Bi\{1 - \theta_{r+1}(0)\}, \quad \theta_{r+1}(\infty) \to 0, \tag{19}$$

$$\phi_{r+1}(0) = 1, \quad \phi_{r+1}(\infty) \to 0, \tag{20}$$

In order to solve the decoupled equations (14)-(17), we use the Chebyshev spectral collocation method. The computational domain $[0, L]$ is transformed to the interval [-1, 1] using $\eta = L(\xi + 1)/2$ on which the spectral method is implemented. Here L is used to invoke the boundary conditions at ∞. The basic idea behind the spectral collocation method is the introduction of a differentiation matrix $\mathcal{D}$ which is used to approximate the derivatives of the unknown variables at the collocation points as the matrix vector product of the form

$$\frac{df_{r+1}}{d\eta} = \sum_{k=0}^{N} \mathbf{D}_{lk} f_r(\xi_k) = \mathbf{D} \mathbf{f}_r, \, l = 0, 1, 2, \dots, N, \tag{21}$$

where $N + 1$ is the number of collocation points (grid points), $\mathbf{D} = 2\mathcal{D}/L$, and $\mathbf{f} = [f(\xi_0), f(\xi_1), \dots, f(\xi_N)]^T$ is the vector function at the collocation points. Higher-order derivatives are obtained as powers of $\mathbf{D}$, that is,

$$f_r^{(p)} = \mathbf{D}^p \mathbf{f}_r, \tag{22}$$

where p is the order of the derivative.

Applying the spectral method to equations (14)-(17), we obtain

$$\mathbf{A}_1 \mathbf{f}_{r+1} = \mathbf{B}_1, \, f_{r+1}(\xi_N) = 0, \tag{23}$$

$$\mathbf{A}_2 \mathbf{p}_{r+1} = \mathbf{B}_2, \, p_{r+1}(\xi_N) = 1, \, p_{r+1}(\xi_0) = 0, \tag{24}$$

$$\mathbf{A}_3 \Theta_{r+1} = \mathbf{B}_3, \, \theta'_{r+1}(\xi_N) = -Bi\{1 - \theta_{r+1}(\xi_N)\},$$

$$\theta_{r+1}(\xi_0) = 0, \tag{25}$$

$$\mathbf{A}_4 \Phi_{r+1} = \mathbf{B}_4, \, \phi_{r+1}(\xi_N) = 1, \, \phi_{r+1}(\xi_0) = 0, \tag{26}$$

where,

$$\mathbf{A}_1 = \mathbf{D}, \, \mathbf{B}_1 = p_r, \tag{27}$$

$$\mathbf{A}_2 = \mathbf{D}^2 + diag(\mathbf{f}_r)\mathbf{D} + diag(-M)\mathbf{I}, \, \mathbf{B}_2 = p_r^2, \tag{28}$$

$$\mathbf{A}_3 = \mathbf{D}^2 + diag(P_r \mathbf{f}_r)\mathbf{D}, \, \mathbf{B}_3 = -[P_r Nb \phi'_r \theta'_r$$
$$+ PrNt \theta'^2_r + PrEc \, p'^2_{r+1} + PrMEc \, p^2_{r+1}], \tag{29}$$

$$\mathbf{A}_4 = \mathbf{D}^2 + diag(Le \mathbf{f}_r)\mathbf{D}, \, \mathbf{B}_4 = -\frac{Nt}{Nb} \theta''_{r+1}, \tag{30}$$

In equations (27)-(30), $\mathbf{I}$ is an identity matrix and $diag[\,]$ is a diagonal matrix, all of size $(N+1) \times (N+1)$ where N is the number of grid points, $\mathbf{f}$, $\mathbf{p}$, Θ and Φ are the values of the functions f, p, θ and ϕ, respectively, when evaluated at the grid points and the subscript r denotes the iteration number.

The initial guesses to start the SRM scheme for equations (14)-(17) are chosen as

$$f_0(\eta) = 1 - e^{-\eta}, \, p_0(\eta) = e^{-\eta}, \, \theta_0(\eta) = \frac{1}{2} e^{-\eta Bi},$$

$$\phi_0(\eta) = e^{-\eta} \tag{31}$$

4. VALIDATION OF RESULTS

The accuracy and robustness of the method have been checked by comparing the SRM results and bvp4c results for various values of Prandtl number P_r and magnetic parameter M which are given in tabular form in Tables 1 and 2. It is clearly seen that both results are in good agreement. It is worthy to mention here that bvp4c is an in-built ODE solver in Matlab. In order to further establish the accuracy of our numerical computations, we have also compared

Table 1 Comparison of SRM results and `bvp4c` results for various values of magnetic parameter *Pr* when *M* = 2, *Le* = 5, *Nb* = 0.1, *Nt* = 0.1, *Bi* = 0.1, and *Ec* = 0.1

Pr	$-f''(0)$	$-\theta'(0)$	$-\phi'(0)$
	SRM results		
1	1.73205081	0.05463367	1.41894254
1.5	1.73205081	0.05489452	1.4354858
2	1.73205081	0.05394962	1.45179315
2.5	1.73205081	0.05252973	1.46769324
3	1.73205081	0.05089058	1.48319372
3.5	1.73205081	0.04914043	1.49834103
	bvp4c results		
1	1.73205081	0.05463367	1.41894254
1.5	1.73205081	0.05489452	1.4354858
2	1.73205081	0.05394962	1.45179315
2.5	1.73205081	0.05252973	1.46769324
3	1.73205081	0.05089058	1.48319371
3.5	1.73205081	0.04914043	1.49834102

Table 2 Comparison of SRM results and `bvp4c` results for various values of magnetic parameter *M* when *Le* = 5, *Nb* = 0.1, *Nt* = 0.1, *Bi* = 0.1, *Ec* = 0.1 and *Pr* = 6.7850

M	$-f''(0)$	$-\theta'(0)$	$-\phi'(0)$
	SRM results		
0	1.00000000	0.07968658	1.58999303
1	1.41421356	0.05731769	1.59321124
2	1.73205081	0.03686300	1.59239387
3	2.00000000	0.01691125	1.58821849
4	2.23606798	-0.00308537	1.58190265
5	2.44948974	-0.02343487	1.57450014
	bvp4c results		
0	1.00000000	0.07968658	1.58999302
1	1.41421356	0.05731769	1.59321123
2	1.73205081	0.03686300	1.59239385
3	2.00000000	0.01691125	1.58821847
4	2.23606798	-0.00308537	1.58190262
5	2.44948974	-0.02343487	1.57450010

Table 3 Computations showing comparison with Makinde and Aziz (2011) for Sh_r when *Le* = 10, *Bi* = 0.1, *Pr* = 10, *Ec* = 0 and *M* = 0

Nt	Nb = 0.1	Nb = 0.2	Nb = 0.3
	Makinde and Aziz (2011)		
0.1	2.2774	2.3109	2.3299
0.2	2.2490	2.3168	2.3569
0.3	2.2228	2.3261	2.3900
0.4	2.1992	2.3392	2.4303
0.5	2.1783	2.3570	2.4792
	Present Results		
0.1	2.2774	2.3109	2.3299
0.2	2.2490	2.3168	2.3569
0.3	2.2228	2.3261	2.3900
0.4	2.1992	2.3392	2.4303
0.5	2.1783	2.3570	2.4792

Table 4 Computations showing comparison with Olanrewaju and Makinde (2013) for Nu_r when *Le* = 10, *Bi* = 0.1, *Pr* = 10, *Ec* = 0 and *M* = 0

Nt	Nb = 0.1	Nb = 0.2	Nb = 0.
	Olanrewaju and Olanrewaju (2013)		
0.1	0.0929	0.0873	0.0769
0.2	0.0927	0.0868	0.0751
0.3	0.0925	0.0861	0.0729
0.4	0.0923	0.0854	0.0703
0.5	0.0921	0.0845	0.0700
	Present Results		
0.1	0.0929	0.0873	0.0769
0.2	0.0927	0.0868	0.0751
0.3	0.0925	0.0861	0.0729
0.4	0.0923	0.0854	0.0703
0.5	0.0921	0.0845	0.0670

the values of reduced Sherwood number Sh_r ($= Re_x^{-1/2} Sh_x$) and reduced Nusselt number Nu_r ($= Re_x^{-1/2} Nu_x$) obtained by Makinde and Aziz (2011) and Olanrewaju and Makinde (2013), respectively with the respective values calculated by the SRM technique. This comparison is presented in Tables 3 and 4 and it has been observed that our results are in full agreement with the results obtained by Makinde and Aziz (2011) and Olanrewaju and Makinde (2013).

5. RESULTS AND DISCUSSION

To study the effect of magnetic field on the nanofluid velocity, the numerical values of the fluid velocity is depicted graphically versus boundary layer parameter η, in Fig. 1, for various values of magnetic parameter. The effects of magnetic parameter *M*, Lewis number *Le*, Brownian motion parameter *Nb*, thermophoresis parameter *Nt*, Biot number *Bi*, Eckert number *Ec* and Prandtl number *Pr* on the nanofluid temperature θ and species concentration φ, within the boundary layer region, are displayed graphically versus boundary layer coordinate η, in Figs. 2 to 7, for various values of pertinent flow parameters. The effects of increase in the values of magnetic parameter *M*, Lewis number *Le*, Brownian motion parameter *Nb*, thermophoresis parameter *Nt*, Biot number *Bi*, Eckert number *Ec*, and Prandtl number *Pr* on the skin friction, which is measured by $f''(0)$, Nusselt number which measures the rate of heat transfer at the plate and can be mea-
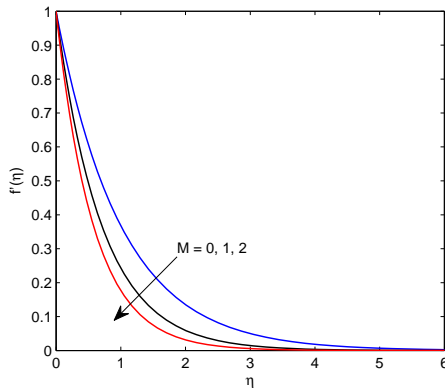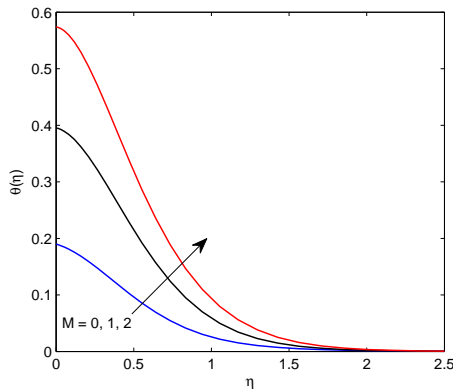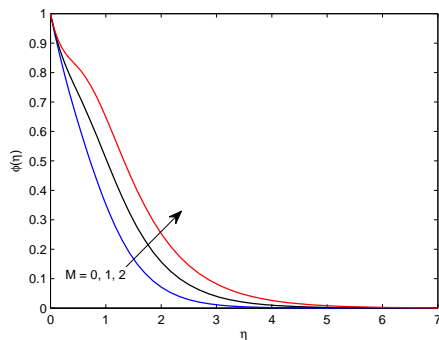
Fig. 1. Effect of magnetic parameter *M* on the fluid velocity f' when $Le = 2$, $Nb = 0.1$, $Nt = 0.1$, $Bi = 0.1$, $Ec = 0.1$ and $Pr = 7$.
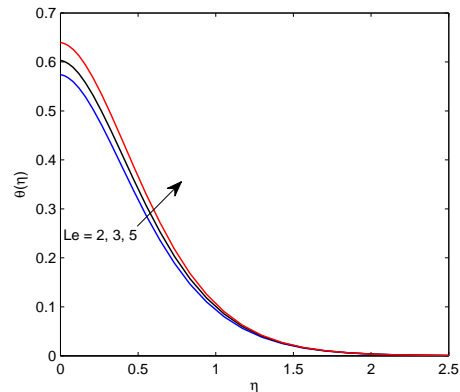

(a)

(b)

Fig. 2. Effect of magnetic parameter *M* on (a) the fluid temperature θ and (b) species concentration φ when $Le = 2$, $Nb = 0.1$, $Nt = 0.1$, $Bi = 0.1$, $Ec = 0.1$ and $Pr = 7$.
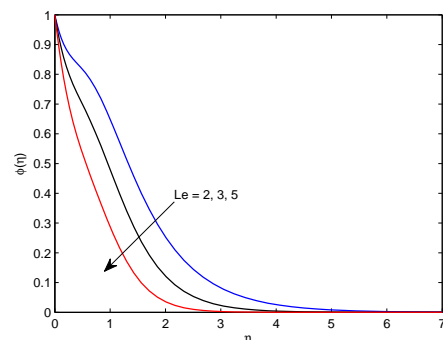
velocity $f'(\eta)$, nanofluid temperature $\theta(\eta)$, and nanoparticle volume fraction $\phi(\eta)$ is depicted in Figs. 1 and 2. An increase in the magnetic field signifies the increase in the resistive force that appears in the flow field due to the applied magnetic field. It is evident from Fig. 1. that the fluid velocity f' decreases on increasing magnetic parameter *M* which implies that the magnetic field reduces fluid velocity in the boundary layer region. Thus the resistive force that appears in the flow field has a tendency to decrease the nanofluid velocity int he boundary layer region. Fig. 2(a) which presents the change in nanofluid temperature with magnetic field is quite important as it reflects the effect of Joulean dissipation on the heat transfer. It is observed that the Joule dissipation has the tendency to significantly increase the nanofluid temperature. Fig. 2(b) demonstrate the influence of magnetic field on the fluid temperature and nanoparticle volume fraction. This implies that magnetic field tends to enhance both fluid temperature and species concentration. Thus
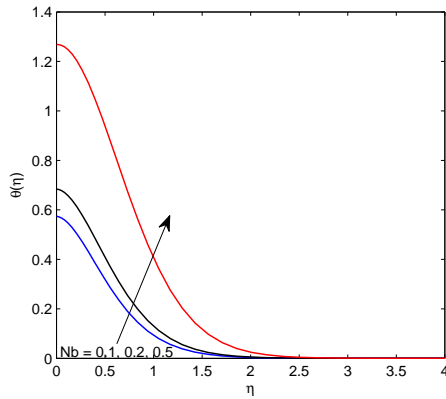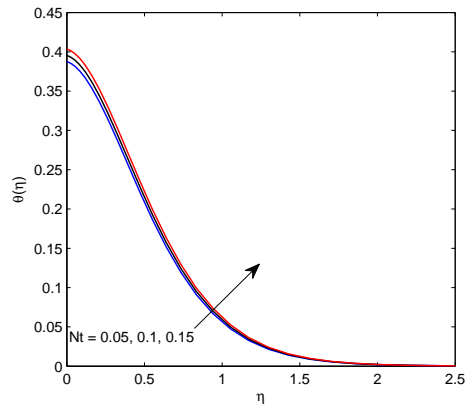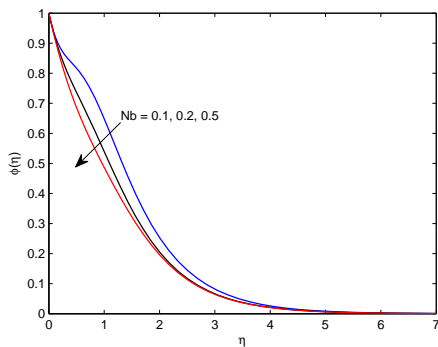

(c)

(d)

Fig. 3. Effect of lewis number *Le* on (a) the fluid temperature θ and (b) species concentration φ when $M = 2$, $Bi = 0.1$, $Ec = 0.1$, $Nb = 0.1$, $Nt = 0.1$ and $Pr = 7$.

sured as variation in $\theta'(0)$ and Sherwood number which measures the rate of mass transfer at the plate and can be measured as a variation in $\phi'(0)$, are presented in Table 5.

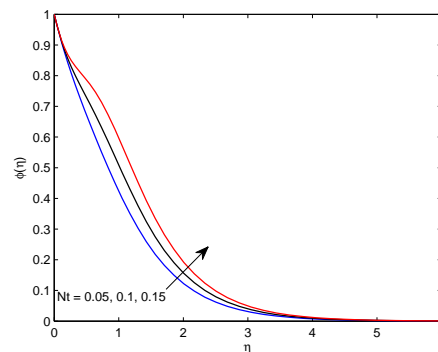The effect of magnetic field *M* on the nanofluid

(e)

(g)

(f)

(h)

Fig. 4. Effect of Brownian motion parameter *Nb* on (a) the fluid temperature θ and (b) species concentration ϕ when *M* = 2, *Bi* = 0.1, *Ec* = 0.1, *Le* = 2, *Nt* = 0.1 and *Pr* = 7.
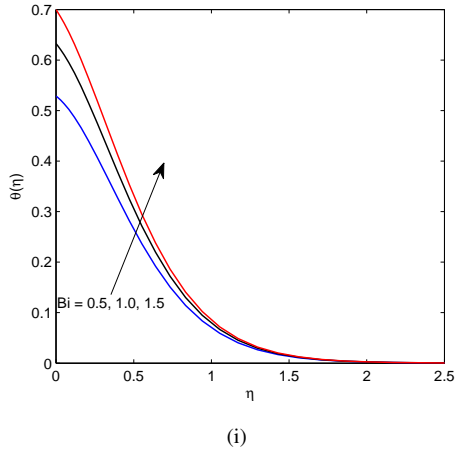
Fig. 5. Effect of Thermophoresis parameter *Nt* on (a) the fluid temperature θ and (b) species concentration ϕ when *M* = 1, *Bi* = 0.1, *Ec* = 0.1, *Le* = 2, *Nb* = 0.1 and *Pr* = 7.

the effect of magnetic field to reduce the fluid velocity results in less transfer of heat from the sheet to the ambient fluid which in turn increases the temperature of the fluid within the boundary layer regime. It is observed that the thickness of the momentum boundary layer decreases while that of thermal and nanoparticle concentration boundary layers increase with the increasing effect of the applied magnetic field.
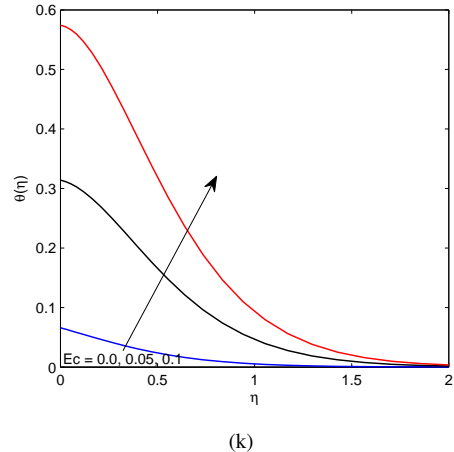
Figures 3(a) and 3(b) are plotted to show the effects of Lewis number *Le* on the nanofluid temperature $\theta(\eta)$ and species concentration $\phi(\eta)$. It is observed from Figs. 3(a) and 3(b) that the effect of Lewis number is to increase the nanofluid temperature whereas it reduces the nanoparticle volume fraction significantly. The Lewis number is the ratio of thermal diffusion to mass diffusion which in turn becomes inversely proportional to mass diffusion, given thermal diffusion is constant. An increase in Lewis number is equivalent to a decrease in mass diffusion and thus it resembles that the nanofluid

temperature decreases while the nanoparticle volume fraction increases with the increase in mass diffusivity. However, the observed effect is more significant on the nanoparticle volume fraction as compared to nanofluid temperature. Both the boundary layer corresponding to nanofluid temperature and nanoparticle concentration are affected by the increase in the mass diffusion in which the effect on the nanoparticle concentration is more significant which gets thicker with the increase in mass diffusion. The thermal boundary layer is respectively less affected and gets thinner when mass diffusion increases.
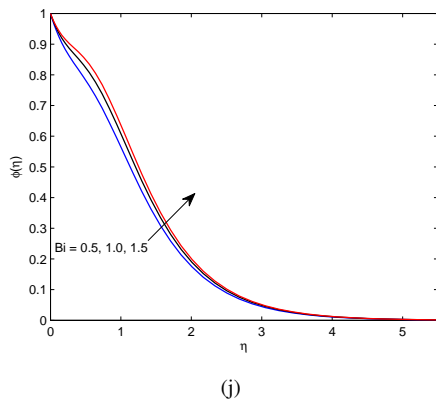
The significant effects of the presence of nanoparticles in the base fluid are due to the Brownian motion and thermophoretic diffusion. Due to Brownian motion, the nanoparticles suspended in a base fluid collide with each other and loses its energy which contribute in the thermal energy of the base fluid while the ther-
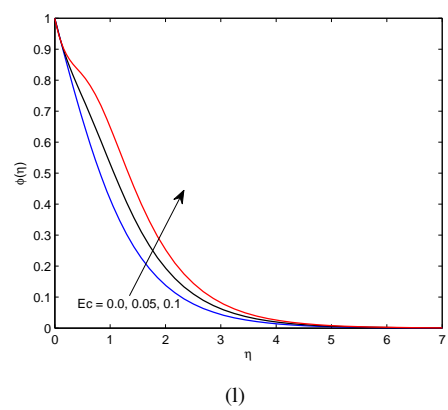
(i)

(j)

Fig. 6. Effect of Biot number *Bi* on (a) the fluid temperature θ and (b) species concentration ϕ when *M* = 1, *Nt* = 0.1, *Ec* = 0.1, *Le* = 2, *Nb* = 0.1 and *Pr* = 7.

(k)

(l)

Fig. 7. Effect of Eckert number *Ec* on (a) the fluid temperature θ and (b) species concentration ϕ when *M* = 2, *Nt* = 0.1, *Bi* = 0.1, *Le* = 2, *Nb* = 0.1 and *Pr* = 7.

mophoretic force is the force which nanoparticle moving away from the hot plate exert on other nanoparticles moving slower. Due to thermophoresis, there is a movement of nanoparticles from the high temperature region to a lower temperature region. The effects of Brownian motion on the nanofluid temperature and nanoparticle volume fraction are presented in Figs. 4(a) and 4(b). It is evident from Figs. 4(a) and 4(b) that fluid temperature increases while the nanoparticle volume fraction decreases on increasing *Nb*. This implies that Brownian motion parameter tends to enhance fluid temperature whereas it has reverse effect on nanoparticle volume fraction. The associated thermal boundary layer increases while the nanoparticle concentration boundary layer decreases with the increase in Brownian motion of the nanoparticles. Figure 5 presents the effects of thermophoresis on the nanofluid temperature and species concentration. It is seen from Figs. 5(a) and 5(b) that the effect of thermophoresis is to

increase the nanofluid temperature ans species concentration within the boundary layer region. These effects are consequences of the thermal energy released due to collision between nanoparticles that take place during Brownian motion and thermophoresis. It is noted that both the associated boundary layers, with the increase in thermophoretic force, get thicker.

The effect of the Newtonian heating process taking place at the surface of the sheet on the nanofluid temperature and nanoparticle volume fraction is depicted graphically in Figs. 6(a) 6(b). The surface of the sheet is subjected to Newtonian heating due to a hot fluid on the other side of the sheet and the strength of this heating process is measured with an increase in the non-dimensional parameter *Bi* (Biot number). It is observed that the an increase in the Biot number brings an increase in the nanofluid temperature and nanoparticle volume fraction. Due to convective heat transfer from the hot fluid to the surface of the sheet, the sheet gets

Table 5 Effects of various parameters on coefficient of skin-friction , Nusselt number and Sherwood number

Le	M	Ec	Nb	Nt	Bi	$-C_f\sqrt{Re_x}$	$Nu/\sqrt{Re_x}$	$Sh/\sqrt{Re_x}$
2	2	0.1	0.1	0.1	0.1	1.73205081	0.04260004	0.85692048
3	2	0.1	0.1	0.1	0.1	1.73205081	0.03970328	1.14559139
5	2	0.1	0.1	0.1	0.1	1.73205081	0.03603953	1.59836809
2	0	0.1	0.1	0.1	0.1	1.00000000	0.08100553	0.90216795
2	1	0.1	0.1	0.1	0.1	1.41421356	0.06046298	0.87898723
2	2	0.1	0.1	0.1	0.1	1.73205081	0.04260004	0.85692048
2	2	0	0.1	0.1	0.1	1.73205081	0.09338748	0.68833179
2	2	0.05	0.1	0.1	0.1	1.73205081	0.06860485	0.77132315
2	2	0.1	0.1	0.1	0.1	1.73205081	0.04260004	0.85692048
2	2	0.1	0.1	0.1	0.1	1.73205081	0.04260004	0.85692048
2	2	0.1	0.2	0.1	0.1	1.73205081	0.03160076	0.82152260
2	2	0.1	0.5	0.1	0.1	1.73205081	-0.02682382	0.80863639
2	1	0.1	0.1	0.05	0.1	1.41421356	0.06123646	0.84996813
2	1	0.1	0.1	0.1	0.1	1.41421356	0.06046298	0.87898723
2	1	0.1	0.1	0.15	0.1	1.41421356	0.05963841	0.91026471
2	1	0.1	0.1	0.1	0.5	1.41421356	0.23566535	0.75484620
2	1	0.1	0.1	0.1	1	1.41421356	0.36752414	0.66222272
2	1	0.1	0.1	0.1	1.5	1.41421356	0.45065440	0.60420352

heated which in turn increases the heat transfer rate from the sheet to the fluid. As a result, the temperature of the fluid gets increased. Thus it follows that the both the boundary layers viz. the thermal boundary layer and the nanoparticle concentration boundary layer get thicker with the increase viscous drag force.

The contribution of the viscous drag on the thermal energy of the nanofluid as well as on nanoparticle volume fraction is presented in Fig. 7(a) and 7(b), respectively. It is observed from these figures that the viscous drag has a significant contribution in increasing the temperature of the nanofluid. The nanoparticle volume fraction also behaves as in increasing function of viscous dissipation. The viscous drag force has the ability to increase the thickness of both thermal and nanoparticle concentration boundary layers.

The effects of various parameters governing the flow field on the coefficient of skin-friction $C_f\sqrt{Re_x}$, Nusselt number $Nu/\sqrt{Re_x}$, and Sherwood number $Sh/\sqrt{Re_x}$ is presented in Table 5. It is observed that magnetic parameter tends to increase the skin friction coefficient whereas it has reverse effect on the Nusselt number and Sherwood number. Thus it follows that the applied magnetic field enhances the skin friction at the surface where as the rate of heat transfer and mass transfer reduce with an increase in the strength of the applied magnetic field. With an increase in Lewis number there is a de-

crease in rate of heat transfer while the rate of mass transfer increase with increasing values of Lewis number. As discussed above, this again follows that the mass diffusion increases the rate of heat transfer while the rate of nanoparticle mass transfer decreases with increase in it. Rate of heat transfer is getting reduced with an increase in Nb and Nt. On the other hand, the rate of mass transfer is getting enhanced with an increase in Nb and Nt. This, in turn, imply that the Brownian diffusion and thermophoretic diffusion of the nanoparticles tend to reduce the rate of heat transfer from the surface whereas these have reverse effect on the rate of nanoparticle mass transfer from the surface of the sheet. Biot number enhances the rate of heat transfer while it reduces the rate of mass transfer. There is a reduction in rate of heat transfer with an increase in viscous dissipation whereas viscous dissipation has reverse effect on rate of mass transfer.

6. CONCLUSIONS

The flow of a viscous, incompressible, and electrically conducting nanofluid past a stretching sheet with Newtonian heating in the presence of a uniform transverse magnetic field is studied taking into account the effects of viscous and Joule dissipations. The spectral relaxation method (SRM) was used to obtain the numerical solution of the governing equations in similarity form which proved to be efficient in handling the solution of the governing equations

as is evident from the comparison results. The numerical solution for the nanofluid velocity, nanofluid temperature, and nanoparticle volume fraction was obtained using the spectral relaxation method. The values of coefficient of skin friction, Nusselt number, and Sherwood number were also obtained. The effects of various physical parameters were studied.It was observed that the effect of applied magnetic field is to decelerate the nanofluid flow whereas to enhance the nanofluid temperature and nanoparticle concentration. The nanofluid temperature gets increased with the increasing effect of Brownian diffusion and thermophoretic diffusion of nanoparticles. However, the nanofluid concentration decreases with Brownian diffusion and increases with increase in thermophoretic diffusion. Newtonian heating and viscous dissipation both contribute toward the enhancement in nanofluid temperature and species concentration. It was further noted that the skin friction at the surface increases with increase in the strength of applied magnetic field. The surface heat transfer is reduced by an increase in Brownian diffusion, thermophoretic diffusion, and viscous dissipation while the surface mass transfer increases with increasing thermophoretic diffusion and viscous dissipation while it decreases with increase in Brownian diffusion.

REFERENCES

Buongiorno, J. and W. Hu (2005). Nanofluid coolants for advanced nuclear power plants. *Proceedings of ICAPP'05, Seoul*, Paper No. 5705.

Chamkha, A. J., A. M. Rashad and E. Al-Meshaiei (2011). m. *Int. J. Chem. Reactor Eng. 9*, A113.

Chen, C. H. (1998). Laminar mixed convection adjacent to vertical, continuously stretching sheets. *Heat Mass Transfer 33*, 471–476.

Choi, S. U. S. (1995). Enhancing thermal conductivity of fluids with nanoparticles. *Proceedings of the 1995 ASME International Mechanical Engineering Congress and Exposition, San Francisco, USA ASME FED 231/MD 66*, 99–105.

Choi, S. U. S., Z. G. Zhang, W. Yu, F. E. Lockwood and E. A. Grulke (2001). Anomalously thermal conductivity enhancement in nanotube suspensions. *Appl. Phys. Lett. 79*, 2252–2254.

Cortell, R. (2005). A note on magnetohydrodynamic flow of a power-law fluid over a stretching sheet. *Appl. Math. Comput. 168*, 557–566.

Cramer, K. and S. Pai (1973). *Magnetofluiddynamics for Engineers and Applied physicists*. McGraw Hill Book Company, New York.

Crane, L. J. (1970). Flow past a stretching plate. *Z. Angrew. Math. Phys. 21*, 645–647.

Das, S. K. and S. U. S. Choi (2009). A review of heat transfer in nanofluids. *Adv. Heat Transfer 41*, 81–197.

Das, S. K., S. U. S. Choi, W. Yu and T. Pradeep (2008). *Nanofluids: Science and Technology*. Wiley, Hoboken, NY.

Erickson, L. E., L. T. Fan and V. G. Fox (1966). Heat and mass transfer on a moving continuous flat plate with suction or injection. *Ind. Eng. Chem. Fund. 5*, 19–25.

Grubka, L. G. and K. M. Bobba (1985). Heat transfer characteristics of a continuous stretching surface with variable temperature. *ASME J. Heat Transfer 107*, 248–250.

Gupta, P. S. and A. S. Gupta (1977). Heat and mass transfer on a stretching sheet with suction or blowing, , 55 (1977), pp. 744-746. *Can. J. Chem. Eng. 55*, 744–746.

Hady, F. M., F. S. Ibrahim, S. M. Abdel-Gaied and M. R. Eid (2012). Radiation effect on viscous flow of a nanofluid and heat transfer over a nonlinearly stretching sheet. *Nanoscale Research Letters 7*, 229.

Ibrahim, W., B. Shankar and M. M. Nandeppanavar (2013). MHD stagnation poiont flow and heat transfer due to nanofluid towards a stretching sheet. *Int. J. Heat Mass Transf. 56*, 1–9.

Ibrahim, W. and B. Shanker (2012). Boundary-layer flow and heat transfer of nanofluid over a vertical plate with convective surface boundary condition. *J. Fluids Eng. 134*, 0812031–8.

Kakac, S. and A. Pramuanjaroenkij (2009). Review of convective heat transfer enhancement with nanofluids. *International Journal of Heat and Mass Transfer 52*, 3187–3196.

Kameswaran, P., P. Sibanda and S. S. Motsa (2013). A spectral relaxation method for thermal dispersion and radiation effects in a nanofluid flow. *Boundary Value Problems 2013*, 242.

Kameswaran, P. K., M. Narayana, P. Sibanda and P. V. S. N. Murthy (2012). Hydromagnetic nanofluid flow due to a stretching or shrinking sheet with viscous dissipation and chemical reaction effect. *Int. J. Heat Mass Transfer 55*, 7587–7595.

Khan, M. S., I. Karim, L. E. Ali and A. Islam (2012). Unsteady MHD free convection boundary-layer flow of a nanofluid along a stretching sheet with thermal radiation and viscous dissipation effects. *Int. Nano Letters 2*(24), 1–9.

Khan, W. A. and I. Pop (2010). Flow near the two-dimensional stagnation point on a infinite permeable wall with a homogeneous-heterogeneous reaction. *Comm. Nonliear. Sci. Numer. Simulat. 15*, 3435–3443.

Kuznetsov, A. V. and D. A. Nield (2010). Natural convective boundar-layer flow of a nanofluid past a vertical plate. *Int. J. Thermal Sci. 49*, 243–247.

Mahapatra, T. R. and A. S. Gupta (2001). Magnetohydrodynamics stagnation point flow towards a stretching shee. *Acta Mech. 152*, 191–196.

Mahapatra, T. R. and A. S. Gupta (2002). Heat transfer in stagnation point flow towards a stretching sheet, heat mass transfer, 38 (2002), pp. 517521. *Heat Mass Transfer 38*, 517–521.

Mahapatra, T. R., S. K. Nandy and A. S. Gupta (2009). Magnetohydrodynamic stagnation point flow of a power-law fluid towards a stretching surface. *Int. J. Non-linear Mech. 44*, 124–129.

Makinde, O. D. and A. Aziz (2011). Boundary layer flow of a nanofluid past a stretching sheet with a convective boundary condition. *Int. J. Thermal Sci. 50*, 1326–1332.

Malvandi, A., F. Hedayati and M. R. H. Nobari (2014a). An analytical study on boundary layer flow and heat transfer of nanofluid induced by a non-linearly stretching sheet. *J. Appl. Fluid Mech. 7*(2), 375–384.

Malvandi, A., F. Hedayati and M. R. H. Nobari (2014b). An HAM analysis of stagnation-point flow of a nanofluid over a porous stretching sheet with heat generation. *J. Appl. Fluid Mech. 7*(1), 135–145.

Meyer, R. C. (1958). On reducing aerodynamic heat-transfer rates by magnetohydrodynamic techniques. *J. Aero. Sci. 25*, 561–572.

Motsa, S. S. and Z. G. Makukula (2013). On spectral relaxation method approach for steady von kárman flow of a reiner-rivlin fluid with joule heating, viscous dissipation and suction/injection. *Cent. Eur. J. Phys. 11*(3), 363–374.

Mustafa, M., T. Hayat, I. Pop, S. Asghar, and S. Obaidat (2011). Stagnation-point flow of a nanofluid towards a stretching sheet. *Int. J. Heat Mass Transfer 54*, 5588–5594.

Nandkeolyar, R., S. S. Motsa and P. Sibanda (2013). Viscous and joule heating in the stagnation point nanofluid flow through a stretching sheet with homogenousheterogeneous reactions and nonlinear convection. *Journal of Nanotechnology in Engineering and Medicine 4*, 04100 1–9.

Nield, D. A. and A. V. Kuznetzov (2009). The cheng-minkowycz problem for natural convective boundary layer flow. *Int. J. Heat Mass Transf. 52*, 5792–5795.

Olanrewaju, A. M. and O. D. Makinde (2013). On boundary layer stagnation point flow of a nanofluid over a permeable flat surface with newtonian heating. *Chem. Eng. Comm. 200*, 836–852.

Parasuraman, L. and V. Chellasamy (2015). MHD flow of nanofluids over an exponentially stretching sheet embedded in a stratified medium with suction and radiation effects. *J. Appl. Fluid Mech. 8*(1), 85–93.

Sakiadis, B. C. (1961). Boundary layer behaviour on continuous solid surface. *A. I. Ch. E. J. 7*, 26–28.

Sreenivasulu, P. and N. Bhaskar Reddy (2015). Lie group analysis for boundary layer flow of nanofluids near the stagnation-point over a permeable stretching surface embedded in a porous medium in the presence of radiation and heat generation/absorption. *J. Appl. Fluid Mech. 8*(3), 549–558.

Vajravelu, K. and T. Roper (1999). Flow and heat transfer in a second grade fluid over a stretching sheet. *Int. J. Non-linear Mech. 34 (6)*, 1031–1036.

Wang, X. Q. and A. S. Mazumdar (2007). Heat transfer characteristics of nanofluids: A review. *Int. J. Thermal Sci. 46*, 1–19.

Xuan, Y. and Q. Li (2003). Investigation on convective heat transfer and flow features of nanofluids. *J. Heat Transfer 125*, 151–155.